Cell Reports

Article

Mis-expression of GATA6 re-programs cell fate during early hematopoiesis

Graphical abstract

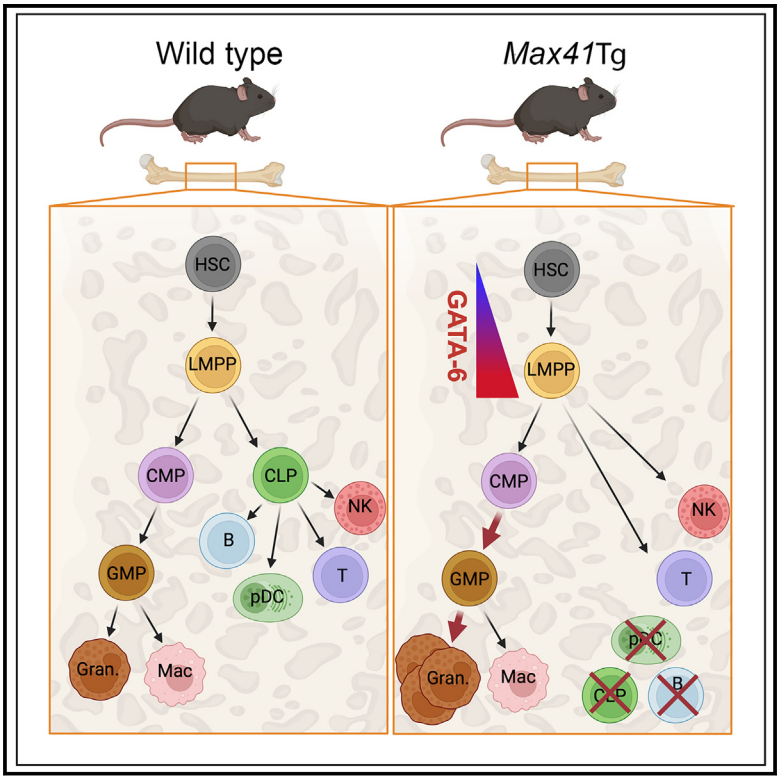

Highlights

- *Max41* mice show excess myelopoiesis at the expense of B cell development
- *Max41* mice lack common lymphoid progenitors (CLPs) but maintain T cell development
- *Max41* allele results in ectopic GATA6 expression in multipotent progenitors
- GATA6 drives myelopoiesis through promoting PU.1 and CEBP/a expression

Authors

Cindy Audiger, Yacine Laâbi, Junli Nie, ..., Jerry M. Adams, Philippe Bouillet, Michaël Chopin

Correspondence

nutt@wehi.edu.au (S.L.N.), strasser@wehi.edu.au (A.S.)

In brief

Audiger et al. show that the inadvertent mis-expression of the transcription factor GATA6 in hematopoietic progenitors results in a loss of common lymphoid progenitors, B cells, and plasmacytoid dendritic cells and instead drives progenitors down the granulocyte-macrophage pathway. Production of T cells was unaffected by loss of common lymphoid progenitors.

Audiger et al., 2024, Cell Reports *43*, 114159
May 28, 2024
https://doi.org/10.1016/j.celrep.2024.114159

CellPress

Cell Reports

CellPress
OPEN ACCESS

Article

Mis-expression of GATA6 re-programs cell fate during early hematopoiesis

Cindy Audiger,[1,2] Yacine Laâbi,[1,2] Junli Nie,[1,2] Leonie Gibson,[1] Julie Wilson-Annan,[1,2,6] Phillip Brook-Carter,[1,2,3] Andrew Kueh,[1,2] Alan W. Harris,[1,2,6] Shalin Naik,[1,2] Stephen L. Nutt,[1,2,*] Andreas Strasser,[1,2,7,*] Jerry M. Adams,[1,2] Philippe Bouillet,[1,2,5] and Michaël Chopin[1,2,4,5]

[1]The Walter and Eliza Hall Institute of Medical Research, Parkville, VIC 3052, Australia
[2]Department of Medical Biology, The University of Melbourne; Melbourne, VIC 3052, Australia
[3]Federation University Australia, Ballarat, VIC 3350, Australia
[4]Department of Biochemistry, Monash Biomedicine Discovery Institute, Monash University, 15 Innovation Walk, Clayton, VIC 3800, Australia
[5]Senior authors
[6]Deceased
[7]Lead contact
*Correspondence: nutt@wehi.edu.au (S.L.N.), strasser@wehi.edu.au (A.S.)
https://doi.org/10.1016/j.celrep.2024.114159

SUMMARY

The traditional view of hematopoiesis is that myeloid cells derive from a common myeloid progenitor (CMP), whereas all lymphoid cell populations, including B, T, and natural killer (NK) cells and possibly plasmacytoid dendritic cells (pDCs), arise from a common lymphoid progenitor (CLP). In *Max41* transgenic mice, nearly all B cells seem to be diverted into the granulocyte lineage. Here, we show that these mice have an excess of myeloid progenitors, but their CLP compartment is ablated, and they have few pDCs. Nevertheless, T cell and NK cell development proceeds relatively normally. These hematopoietic abnormalities result from aberrant expression of *Gata6* due to serendipitous insertion of the transgene enhancer (*Eμ*) in its proximity. *Gata6* mis-expression in *Max41* transgenic progenitors promoted the gene-regulatory networks that drive myelopoiesis through increasing expression of key transcription factors, including PU.1 and C/EBPa. Thus, mis-expression of a single key regulator like GATA6 can dramatically re-program multiple aspects of hematopoiesis.

INTRODUCTION

The cellular differentiation pathways by which the diverse types of blood cells arise from a hematopoietic stem cell (HSC) has received intense attention.[1,2] The HSC resides in the so-called LSK (lineage marker-negative Sca-1$^+$ cKit$^+$) fraction, which can be further subdivided into multipotent progenitor fractions 1–4 (MPP1–MMP4).[3] Mature hematopoietic cells are traditionally separated into two distinct branches: lymphoid and the myeloid. The major types of lymphoid cells are T, B, and innate lymphoid cells, such as natural killer (NK) cells. The myeloid lineage comprises many different subtypes, including granulocytes, monocytes, macrophages, conventional dendritic cells, erythrocytes, and megakaryocytes. The two lineages were long thought to represent entirely distinct differentiation pathways. This concept was supported by the isolation of common lymphoid progenitors (CLPs), thought to produce all types of lymphoid cells but no myeloid cells,[4] and common myeloid progenitors (CMPs), which generate all types of myeloid cells, but no lymphoid cells.[5] However, advances in flow cytometry approaches and the identification of specific markers of early hematopoietic progenitor subpopulations have revealed numerous intermediary stages in both the lymphoid and myeloid cell differentiation trajectories.[1] Also, there is evidence that certain hematopoietic progenitor populations can differentiate along either the lymphoid or the myeloid lineage.[6]

Consequently, the discovery in 1994 of a transgenic mouse strain, *Max41*, in which excessive granulocytes appeared to originate from B cell precursors, promised to provide a unique *in vivo* window on the lineage potential of hematopoietic progenitor populations.[7] The striking lineage deviation in the *Max41* mice was shown to originate early in the fetal liver and appeared to be intrinsic to the hematopoietic system, since transfer of *Max41* bone marrow cells could install the phenomena in recipient wild-type mice. Here, we identify other important hematopoietic abnormalities in this strain and uncover the genetic basis for its remarkable phenotype.

RESULTS

Multiple perturbations of hematopoietic cell differentiation in *Max41* transgenic mice

In the *Max41* transgenic mouse strain, the insertion of an *Eμ-Max* transgene (Figure S1A) failed to overexpress a *Max* transcript but provoked a remarkable lineage deviation of B cell precursors to granulocytes that has been described in detail.[7] In heterozygous *Max41*$^{T/+}$ animals, pro-B, pre-B, and mature B lymphocyte populations are nearly absent, while granulocyte numbers are

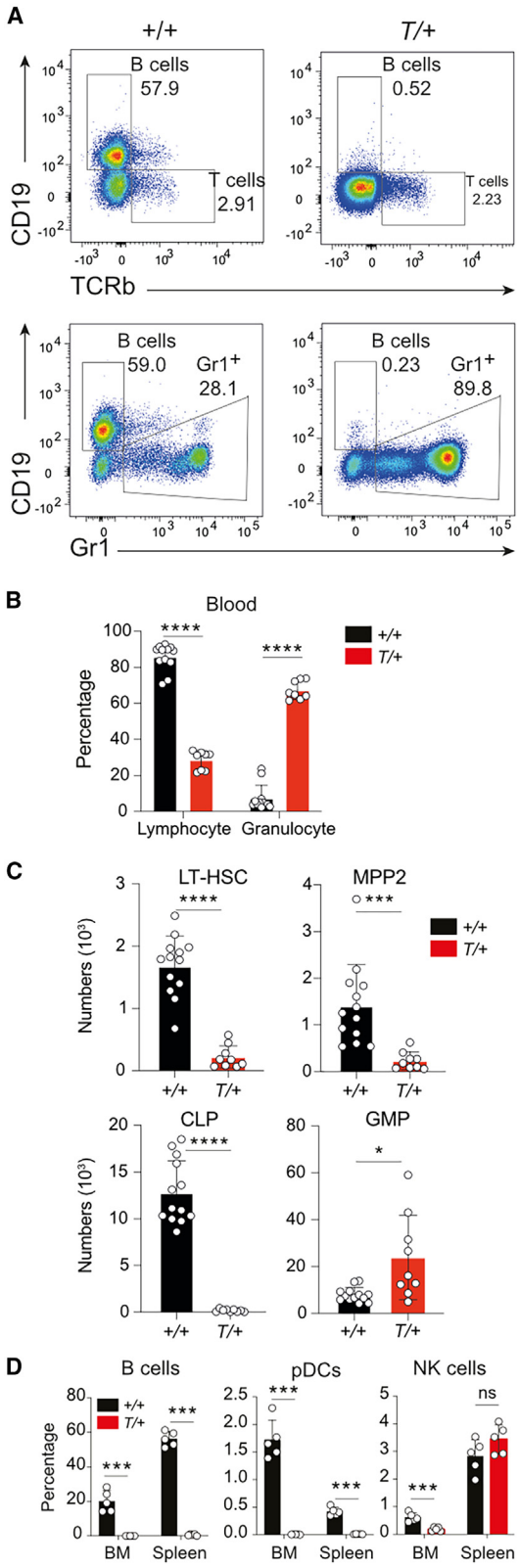

Figure 1. Multiple alterations in the hematopoietic system of *Max41* transgenic mice

(A) Characteristic fluorescence-activated cell sorting (FACS) plots showing the populations of B cells and granulocytes in the white blood cells of WT (+/+) and *Max41* transgenic (T/+) mice.

(B) Decrease of lymphocytes and increase in granulocytes in the blood of *Max41* transgenic mice (T/+) compared to their WT (+/+) littermates as determined by an Advia blood analyzer (n = 8–12 mice per genotype).

(C) Marked decrease in LT-HSC, MPP2 and CLP hematopoietic progenitor cell populations but a slight increase in the GMP population in the bone marrow of *Max41*$^{T/+}$ mice as determined by flow cytometry.

(D) Quantitation of the frequency of B cells, pDCs, and NK cells in the bone marrow and spleen of *Max41*$^{T/+}$ and WT (+/+) mice (n = 5 mice per genotype).

(B–D) Graphs show the mean ± SEM, with each dot depicting the value from an individual mouse. ****p < 0.0001, ***p < 0.001, *p < 0.05 using an unpaired Student's t test with Welch's correction.

See also Figures S1 and S2.

greatly increased (Figures 1A and 1D). This phenotype has been stable over >40 generations, and mice are routinely genotyped using an Advia 2120i blood analyzer (Bayer) (Figure 1B). Furthermore, the spleens of the *Max41* animals are enlarged and have an abnormal architecture, reflecting reduced white pulp and an invasion of granulocytes (Figure S1B). The bones are unusually pale because their marrow is replete with mature granulocytes (Figure S1C).

Hematopoietic stem and progenitor cell (HSPC) populations in the bone marrow of *Max41* mice showed notable differences from those in wild-type (WT) mice (Figures 1C and S2). Their most striking features (Figure 1C) were the marked reduction of long-term (LT)-HSCs and MPP2s and the nearly complete absence of CLPs (~50-fold decrease). Concomitantly, granulocyte/monocyte progenitors (GMPs) were increased ~3-fold (Figure 1C).

CLPs have been reported to be precursors not only for B, T, and NK cells[4] but also of plasmacytoid dendritic cells (pDCs).[8] In line with this, pDCs were virtually absent in *Max41* mice (Figure 1D). Remarkably, however, thymopoiesis (Figure S1D) and peripheral NK cell numbers were unaltered in *Max41*$^{T/+}$ mice when compared to age-matched WT controls (Figure 1D).

While the absence of CLPs explains the marked decrease in B cells in *Max41* mice, the normal numbers of T cells and NK cells may seem surprising. However, it has been proposed that CLPs are not the physiological progenitors of T cells and that a less mature sub-population of MPP4 cells, termed lymphoid-primed multipotent progenitors (LMPPs), can give rise to both T cells and group 2 innate lymphoid cells (ILC2s) more efficiently than CLPs.[9] Although NK cell ontogeny is widely considered to be exclusively lymphoid and dependent on CLPs,[10] certain myeloid progenitor populations also possess some NK potential.[11–13] Thus, the presence of NK cells at normal levels in *Max41* mice supports a CLP-independent origin for these cells. pDCs have been proposed to differentiate from both the myeloid and the lymphoid arms through a convergent pathway;[14,15] however, recent studies have argued that pDCs predominantly derive from CLPs.[8,16] In line with the latter studies, the numbers of pDCs in *Max41* mice were substantially reduced, despite these animals having normal numbers of common DC progenitors (CDPs), originally described as a source of pDCs (Figure S2).[17,18] Thus, our results support the

notion that CLPs represent the major source of pDCs *in vivo*, although an independent impact of the *Max41* mutation on pDC development cannot be excluded.

While the alterations in the B lymphoid and granulocyte populations were the first anomalies discovered in *Max41* transgenic mice,[7] the additional alterations that our present study has uncovered suggest that the mutation has a more complex impact on hematopoietic cell development than previously thought and highlight the potential of this model to help delineate the complex relationships between different hematopoietic progenitor populations and the origins of the various mature hematopoietic cell subsets. The *Max41* phenotype is dominant, suggesting that it reflects inappropriate activation of a gene, but the genetic basis of this hematopoietic differentiation anomaly has remained elusive to date.

Multiple rearrangements in a chromosome 18 region are linked to the *Max41* phenotype

To simplify the molecular analysis, transgenic animals were kept in the hemizygous state by systematic crossing of a *Max41* animal with a WT C57BL/6 mouse. The *Max41* transgene contains the $E\mu$ enhancer from the immunoglobulin heavy-chain gene locus, which is activated very early in lymphoid differentiation, coupled to the *Max* gene, which encodes a heterodimeric partner of the transcription factor MYC (Figure S1A). Since the *Max* transgene is silent in *Max41* mice, their remarkable phenotype has been proposed to reflect inadvertent insertion of the transgene in the vicinity of an endogenous gene that impacts hematopoiesis.[7] We have characterized the insertion sites by making and screening libraries of large *Max41* DNA fragments for clones bearing SV40 tag sequences from the transgene. These analyses revealed unexpected complexity with multiple rearrangements and four insertion sites but all falling within a 286-kb region of chromosome 18 that lies 11.2 Mb from its centromere (Figure S3). Surprisingly, no known coding genes lie within this 286-kb region, and, to our knowledge, no spliced expressed sequence tags have been assigned to it, nor any microRNAs (miRNAs) or long non-coding RNAs. The rearrangements include insertion of a concatemer of 6–10 transgenes, a single transgene insert, two inserts of transgene fragments, inversion within a 120-kb segment, deletions of 2 kb and 51 kb, and integration of a 13.3-kb fragment from chromosome 5 (Figure S3). All these rearrangements are genetically linked to the *Max41* phenotype because none have segregated during more than 40 generations of backcrossing the *Max41* transgenic mice onto the C57BL/6 genetic background.

The 13.3-kb segment from chromosome 5 seemed of particular interest because it contained exons of two known genes, *Znhit1* and *Cldn15*, that were included in two different chimeric transcripts that could be detected specifically in bone marrow cells from *Max41* mice (Figure 2A; data not shown). To test whether either chimeric transcript contributed to the *Max41* phenotype, we deleted the *Znhit1* or *Cldn15* exons from the transgenic locus (Figure 2B) using CRISPR.[19] However, the animals harboring either of these gene deletions retained severe reductions in B cells and increases in granulocytes akin to the original *Max41* mice (Figure 2C).

Gata6 is abnormally expressed in bone marrow cells from *Max41* transgenic mice

Having ruled out the truncated *Znhit1* and *Cldn15* genes in the transgenic region as the cause of the *Max41* phenotype, we then considered that the potent $E\mu$ enhancer within the transgenic locus in multiple copies might have activated a chromosome 18 gene more distal from the insertion site. The closest gene on the 5′ side of the transgenic region is *Gata6*, located ~110 kb upstream, while the closest gene 3′ of the insertion region is *Rbbp8*, 350 kb downstream (Figure 3A). Two additional genes, *Abhd3* and *Mib1*, lie 5′ to *Gata6* on chromosome 18.

To test whether the transgene insertion had affected the expression of any of these genes, we performed RT-PCR on RNA from total bone marrow cells from a WT (+/+) and a *Max41* transgenic (T/+) mouse. The signals for *Abhd3*, *Mib1*, and *Rbbp8* were very similar between WT and *Max41* bone marrow cells, showing that the transgenic rearrangements did not alter their expression. In striking contrast, *Gata6* was not expressed in WT bone marrow cells (as expected from the Immgen database; Figure S4A), but it yielded a strong signal in bone marrow cells from the *Max41* transgenic mice (Figure 3B). To confirm and extend this finding, we monitored *Gata6* expression by real-time qPCR across a range of hematopoietic progenitor cell populations as well as peritoneal macrophages, a positive control known to express *Gata6*. This revealed that *Gata6* was expressed in hematopoietic progenitors from *Max41* mice but not in their WT counterparts (Figure 3C).

To perform an unbiased assessment of *Gata6* expression in mouse bone marrow cells, we interrogated single cell RNA sequencing (scRNA-seq) data from the Tabula Muris Compendium.[20] This analysis confirmed the absence of expression of *Gata6* in any mouse bone marrow cell population, in contrast to the related family members *Gata1*, *Gata2*, and *Gata3*, which were readily detected in $Cd34^{+}$ hematopoietic progenitor populations in the same samples (Figures S5A–S5B). The absence of *Gata6* expression was not due to the lower sensitivity of single-cell RNA-seq, as we were able to robustly detect *Gata6* transcripts in mouse heart tissue from the same database (Figure S5C).

Gata6 mis-expression is responsible for the *Max41* phenotype

To determine whether GATA6 is responsible for the hematopoietic abnormalities in *Max41* mice, we designed CRISPR guide RNAs to delete *Gata6* exon 2 and thereby generate a null allele on the $Max41^{T/+}$ genetic background. Because *Gata6*-deficient mice (−/−) die between embryonic day 5.5 and 7.5 due to a defect in endoderm differentiation, born transgenic animals harboring the *Gata6*-null mutation are obligate heterozygotes at the *Gata6* locus and, hence, carry the null mutation on either the WT chromosome 18 allele (*trans* configuration) or the transgenic allele (*cis* configuration) (Figure 3D).[21,22] While alleles in the *trans* configuration segregate independently, those in the *cis* configuration are linked and segregate together. The breeding strategy used to generate mice of the different genotypes is shown in Figure S6.

To test the involvement of *Gata6* in the *Max41* hematopoietic defects, we generated $Gata6^{+/-}$ *T*/+ (*trans*) and $Gata6^{+/-}$

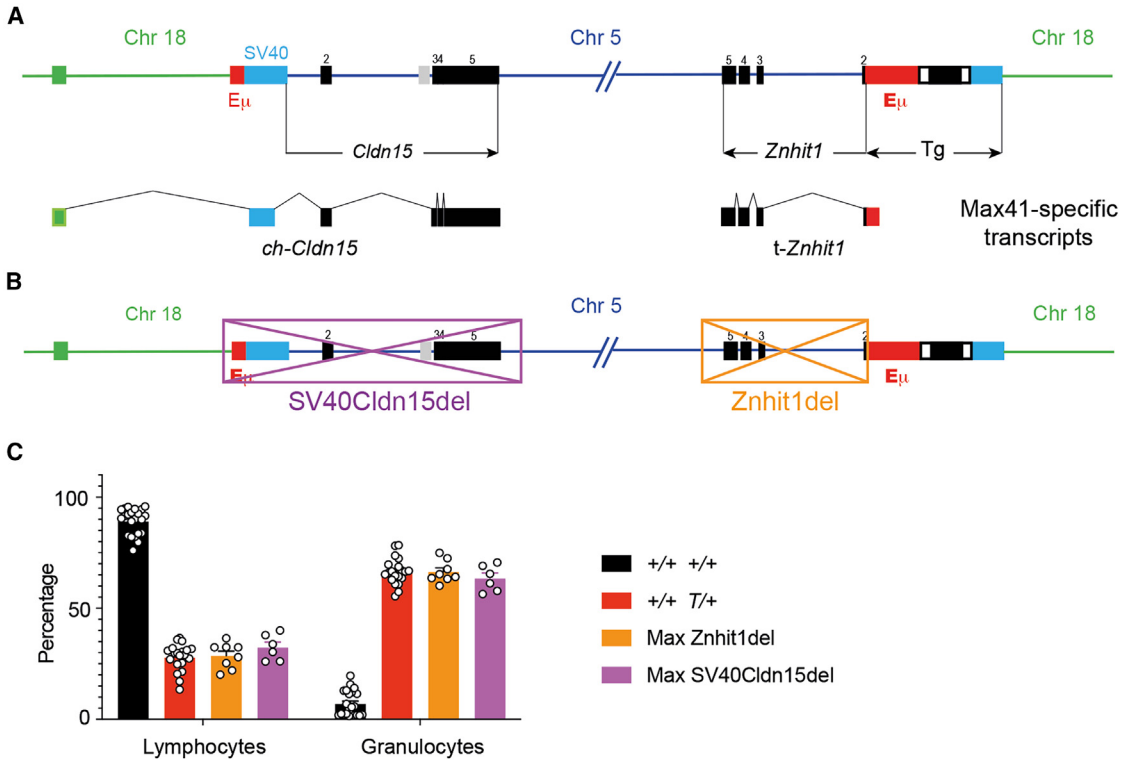

Figure 2. Two chimeric transcripts involving chromosome 5 exons have no role in the *Max41* phenotype

(A) Insertion during transgenesis of a 13.3-kb fragment of chromosome 5 into chromosome 18 generates two chimeric transcripts expressed uniquely in *Max41* transgenic mice.

(B) Deletions of *Cldn15* exons (purple box) or *Znhit1* exons (orange box) in the translocated chromosome 5 region to assess the role of each chimeric transcript in the *Max41* phenotype.

(C) Blood analysis shows that animals with the deletion of exons from either *Cldn15* (Max SV40Cldn15del) or *Znhit1* (Max Znhit1del) retain the marked decrease in B lymphocytes and increase in granulocytes characteristic of the *Max41* phenotype. The graph shows the mean ± SEM, with each dot depicting the value from an individual mouse (n = at least 6 for each genotype).

See also Figure S3.

T/+ (*cis*) animals and compared the composition of their hematopoietic system. The *Gata6*$^{+/-}$ *T*/+ (*trans*) mice still showed the *Max41* phenotype in the spleen (Figures 3E and 3G), blood (Figure 3F), and bone marrow (Figures 3E and 3G), including in their hematopoietic progenitor cell populations (Figure 4A). In striking contrast, the *Gata6*$^{+/-}$ *T*/+ (*cis*) mice had numbers and proportions of lymphoid and myeloid cells comparable to WT mice (Figures 3E–3G) and a spleen of normal size, structure, and composition (data not shown). Notably, all hematopoietic progenitor cell populations, B cells, and pDCs were restored to WT levels in the *Gata6*$^{+/-}$ *T*/+ (*cis*) animals (Figures 4A and 4B). Thus, we found no significant difference between WT and *Gata6*$^{+/-}$ *T*/+ (*cis*) animals, demonstrating that the inappropriate *Gata6* expression evoked by the transgene insertions is responsible for the entire *Max41* phenotype. Importantly, the ablation of the *Max41* phenotype in the mice with the *Gata6* null mutation on the transgenic allele (in *cis*), but not those with it on the non-transgenic allele (in *trans*), is precisely what is expected from enhancer-induced activation of this chromosome 18 gene by an enhancer within the transgenic locus—almost certainly *Eμ*.

Gata6 mis-expression in hematopoietic progenitors drives the myeloid gene expression program

To begin to understand why *Gata6* mis-expression had such a pronounced impact on hematopoiesis, we performed gene expression analysis on sorted progenitors from WT and *Max41*$^{T/+}$ mice. The *Eμ* enhancer is predicted to promote gene expression in a subset of MPPs, CMPs, CLPs, and all subsequent stages of B cell development. As CLPs and B cells are absent from *Max41*$^{T/+}$ mice (Figure 1), we instead sorted the LSK fraction that encompasses MPP1–MMP4 as well as the CMP population and performed bulk whole transcriptome RNA-sequencing (RNA-seq). Comparison of the LSK and CMP groups from each population revealed that there were many more differentially expressed genes between WT and *Max41*$^{T/+}$ CMPs (300 upregulated and 351 downregulated) compared to the same comparison using LSKs (88 upregulated and 5 downregulated) (Figure 5A). 44% of the genes up-regulated in WT LSK cells (39 of a total of 88) were also upregulated in *Max41*$^{T/+}$ CMPs (Figure 5B). In keeping with our prediction, *Gata6* was transcribed at background rates in the WT LSK and CMP fractions but was clearly transcriptionally activated in both cell populations derived

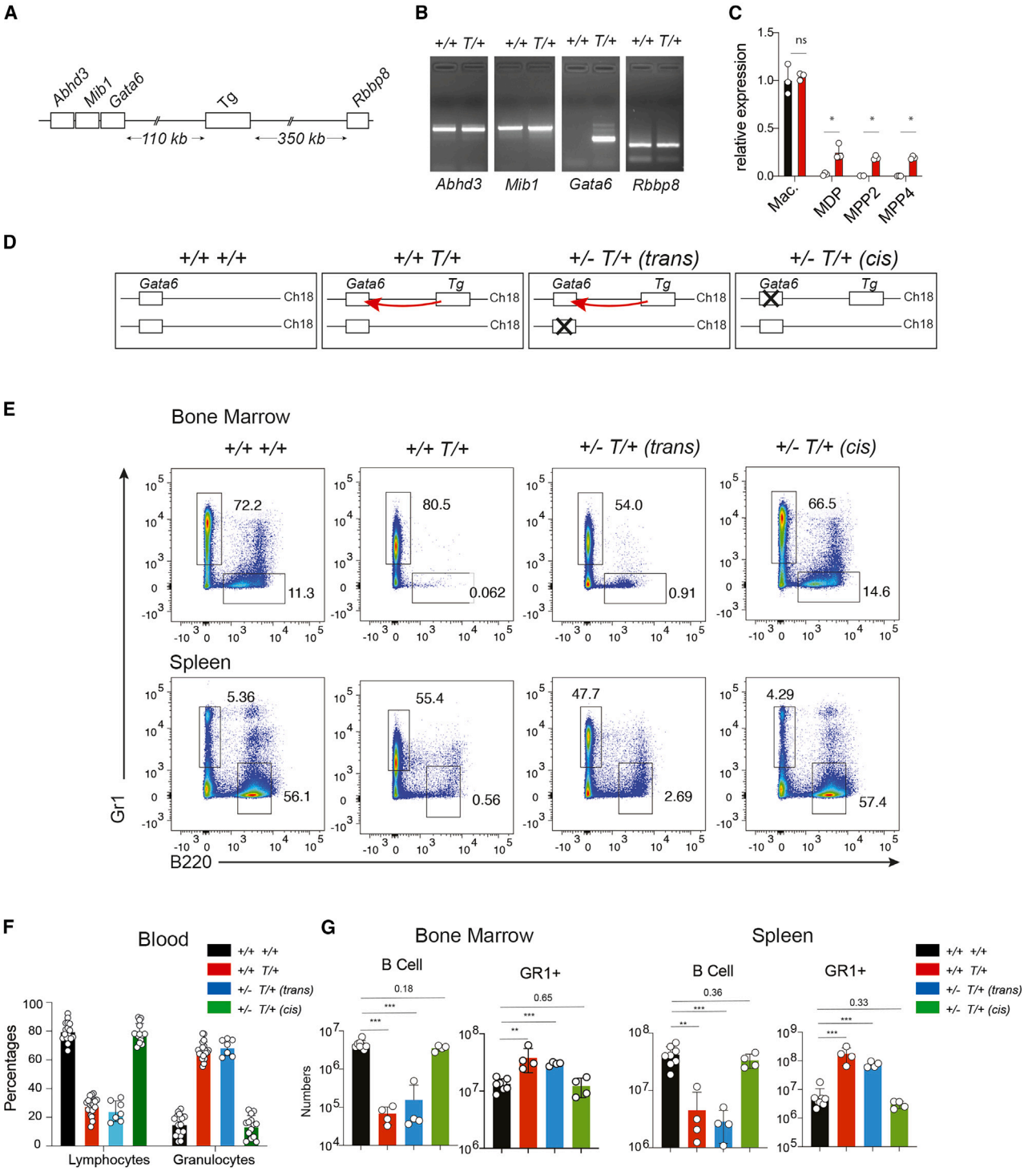

Figure 3. *Gata6* mis-expression is required for the *Max41* phenotype

(A) The region of transgene insertion lies between *Gata6* and *Rbbp8* on chromosome 18. Other nearby genes, *Mib1* and *Abhd3*, are also indicated.

(B) RT-PCR on total bone marrow RNA of WT (+/+) and transgenic (*T*/+) *Max41* mice for the expression of the indicated genes.

(C) RT-qPCR for the expression of *Gata6* in peritoneal macrophages (Macs) and MDPs (monocyte/dendritic cell progenitors), MPP2 and MPP4 isolated from the bone marrow of *Max41* transgenic mice (T/+), and WT (+/+) littermates. Data were normalized to *Gapdh* and are shown as mean relative expression ± SEM from triplicate samples (shown as dots). The mean value for a single +/+ Mac sample was arbitrarily set to 1.

(legend continued on next page)

from *Max41*$^{T/+}$ bone marrow, with expression being most pronounced in the CMP fraction (Figure 5C). Interestingly, we observed downregulation of *Gata1* and *Gata2* in LSKs and CMPs from *Max41*$^{T/+}$ mice, potentially suggesting a compensatory response to mis-expressed *Gata6* (Figure S4C). These RNA-seq data also confirmed that the expression of the flanking genes, *Mib1* and *Rbbp8*, was unaltered in the *Max41*$^{T/+}$ LSKs and CMPs (Figure S4D). *Abhd3* was not expressed in LSKs or CMPs from either genotype (data not shown).

Gene set enrichment analysis revealed that the *Max41*$^{T/+}$ CMPs were strongly enriched for genes that are characteristic for granulocytes and macrophages (Figure 5D). The differentially expressed genes included the enzyme *Mpo* and *Spi1* (*PU.1*) and *Cebpa* and *Cebpd,* key transcription factors that are well known for their ability to drive myelopoiesis[24,25] (Figure 5E). Taken together, these findings demonstrate that mis-expression of GATA6 drives a gene-regulatory program that orchestrates enhanced myelopoiesis and that this ectopic program is already apparent at the CMP stage of hematopoiesis.

DISCUSSION

Since the initial description of the remarkable *Max41* phenotype in 1994,[7] much energy has been expended characterizing the multiple genomic rearrangements acquired during the transgene insertion. The recent advances in CRISPR technology[19] enabled the present study to identify the responsible gene. Our finding that deletion of *Cldn15* or *Znhit1* exons from the transgenic locus did not rescue the *Max41* phenotype (Figure 2C) prompted us to look farther afield on chromosome 18. Indeed, the nearest gene, *Gata6*, was abnormally upregulated in bone marrow hematopoietic progenitor cells from *Max41* transgenic mice. Significantly, the entire *Max41* phenotype was rescued by a null mutation in *Gata6* engineered to lie on the same allele as the transgenes (in *cis*), whereas the same null mutation on the non-transgenic allele (in *trans*) had no impact. These findings provide compelling genetic evidence that the *Max41* phenotype is caused by aberrant activation of *Gata6* expression owing to insertion in its vicinity of the transgenic enhancer, *Eμ*. Thus, these results suggest that most of the genomic rearrangements in *Max41* (e.g., the deletions, inversions, and a translocation) have no relevance to the phenotype, except for placing the *Eμ* enhancer in the general proximity of *Gata6*.

Interestingly, multiple lines of evidence, including bulk and single-cell RNA-seq revealed that *Gata6* is not normally expressed in bone marrow hematopoietic progenitors. In the hematopoietic system, GATA6 expression is normally limited to peritoneal macrophages.[26–28] By contrast, the related transcription factors GATA1, GATA2, and GATA3 are known to play essential roles in the development and maintenance of the hematopoietic system, and mutations that alter their expression have been linked to several hematological disorders.[29] Nevertheless, because all GATA transcription factors recognize and bind to the WGATAR motif, inappropriate expression of GATA6 during hematopoiesis may well alter the fate of certain hematopoietic progenitor cell populations. Of note, none of the GATA factors are highly expressed in CLPs, but *Gata2* and *Gata3* are expressed in MPP4 cells, the precursors of CLPs (Figure S4B). Hence, the normal transition from the MPP4 (also known as LMPP) to the CLP stage may require low GATA factor activity, which is precluded in *Max41* transgenic mice by *Eμ* enhancer-driven Gata6 (Figure 5). Pertinently, ectopic expression of GATA1, GATA2, or GATA3 in multipotent *Pax5*$^{-/-}$ pro-B cells rapidly generates granulocyte/macrophage lineage cells *in vivo*.[30] In keeping with this, our RNA-seq analysis revealed that ectopic GATA6 expression in CMPs resulted in increased expression of myeloid genes, including those encoding key transcription factors, such as PU.1 (*Spi1*) and C/EBP-family genes (*Cebpa* and *Cebpd*), which have been shown to promote myelopoiesis when mis-expressed.[31,32] Collectively, these results suggest that the *Eμ* enhancer, which is active at the very onset of lymphopoiesis, drives an aberrant pulse of GATA6 in MPPs that re-directs these progenitors to the granulocyte/macrophage pathway (Figure 6).

While the alterations in the B cell and granulocyte populations were the first abnormalities discovered in *Max41* mice,[7] the additional notable hematopoietic perturbations affecting multiple progenitor cell subsets described here reveal the complex impact of this mutation on hematopoiesis. For example, our findings that T cells and NK cells appear relatively unaffected by the absence of CLPs in *Max41* mice suggests that their production can be independent of this progenitor cell population, as suggested by some other studies in intact mice[9,33] and in mice lacking the transcription factor Ikaros.[33] Although it is undoubtedly the consensus in the field that NK cells develop from CLPs,[10] there are several studies that raise the possibility of a myeloid-derived NK cell pathway.[11–13] By contrast, the absence of pDCs in *Max41* mice supports the concept that CLPs are the main (possibly the sole) source of pDCs *in vivo*. These findings illustrate the potential of this fascinating mouse model and will be made freely available to help unravel the intricacies of hematopoietic cell development and its molecular control.

Limitations of the study

This study shows that random incorporation of a transgene into the mouse genome has, by serendipity, created a remarkable *in vivo* model of lineage switching in the hematopoietic system

(D) Illustration showing that the *Gata6*-null mutation and transgene (*Tg*) insertion can be either on the same chromosome 18 allele (in *cis*) or on the opposite allele (in *trans*).
(E) Distribution of B220$^+$ B cells and Gr1$^+$ granulocytes in the bone marrow and spleens of *Gata6*$^{+/+}$ +/+, *Gata6*$^{+/+}$ *T*/+, *Gata6*$^{+/-}$ *T*/+ (*trans*), and *Gata6*$^{+/-}$ *T*/+(*cis*) mice, as determined by flow cytometry analysis. Data are representative of at least 4 independent biological replicates for each genotype.
(F) Mean percentages ± SEM of lymphocytes and granulocytes in the blood of *Gata6*$^{+/+}$ *Max41*$^{+/+}$, *Gata6*$^{+/+}$ *Max41*$^{T/+}$, *Gata6*$^{+/-}$ *Max41*$^{T/+}$ (*trans*), and *Gata6*$^{+/-}$ *Max41*$^{T/+}$(*cis*) mice (n = 7–20 mice per genotype).
(G) Mean numbers ± SEM of B cells and granulocytes (CD11b$^+$Gr1$^+$) in the bone marrow of *Gata6*$^{+/+}$ *Max41*$^{+/+}$, *Gata6*$^{+/+}$ *Max41*$^{T/+}$, *Gata6*$^{+/-}$ *Max41*$^{T/+}$ (*trans*), and *Gata6*$^{+/-}$ *Max41*$^{T/+}$(*cis*) mice (n = at least 4 for each genotype).
Each dot in (C), (F), and (G) comes from an independent mouse. ***$p < 0.001$, **$p < 0.01$, *$p < 0.05$ or as indicated using an unpaired Student's t test with Welch's correction. See also Figures S4 and S5.

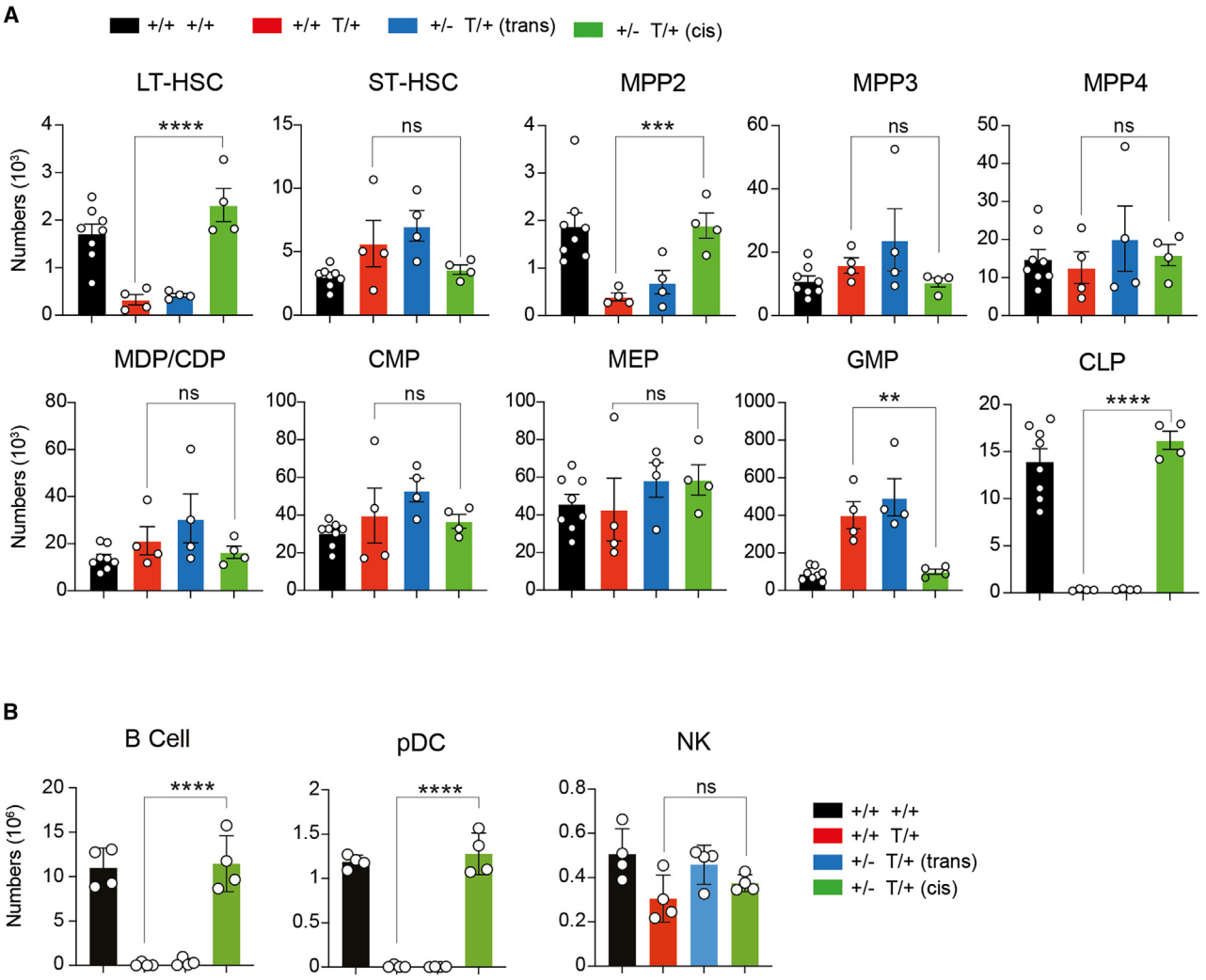

Figure 4. Deletion of *Gata6* from the *Max41* transgenic allele abrogates the *Max41* phenotype

(A) Analysis of the indicated hematopoietic stem or progenitor cell populations and B lymphoid cell types in *Gata6*$^{+/+}$ *Max41*$^{+/+}$, *Gata6*$^{+/+}$ *Max41*$^{T/+}$, *Gata6*$^{+/-}$ *Max41*$^{T/+}$ (*trans*), and *Gata6*$^{+/-}$ *Max41*$^{T/+}$(*cis*) mice ($n = 4$ per group). Significant drops were seen in the LT- and ST-HSC and the MPP2 early progenitors and CLP, whereas numbers of GMP were elevated severalfold.

(B) Normal numbers of pDCs and NK cells in the bone marrow of *Gata6*$^{+/-}$ *Max41*$^{T/+}$(*cis*) mice.

Data show one representative experiment with $n = 4$ per genotype. Each dot comes from an independent mouse. Gating strategies and antibodies are described in Figure S2 The p values compare the *Gata6*$^{+/+}$ *Max41*$^{T/+}$ and *Gata6*$^{+/-}$ *Max41*$^{T/+}$(*cis*) groups using an unpaired Student's t test with Welch's correction. ****$p < 0.0001$, ***$p < 0.001$, **$p < 0.01$; ns, not significant, $p > 0.05$.

driven by mis-expression of a predominantly non-hematopoietic GATA-family member, GATA6. We do not as yet have a detailed molecular model for the phenomena observed but propose that transient GATA6 activity in MPPs sets in train a process that promotes myelopoiesis through increased PU.1 and C/EBPa activity. scRNA-seq analysis of the hematopoietic compartment of *Max41* mice would be required to further define the lineage switching process observed in this study. Whether the ectopic GATA6 acts as a surrogate for one of the other GATA family members remains to be determined, as does identification of the precise transcriptional targets of GATA6.

Although our evidence to date suggests that GATA6 is not active in any bone marrow hematopoietic progenitor, and, thus, that the lymphoid-to-myeloid lineage skewing is a product of mis-expression, we cannot exclude the possibility that this process does occur physiologically, as the existence of bipotent lymphoid/myeloid progenitors has been claimed for both fetal liver and adult bone marrow.[34–36] Careful analysis of a timed scRNA-seq dataset from fetal hematopoiesis would directly address this issue. Finally, while we speculate that GATA6 blocks the development of B cells and pDCs through its role in inhibiting the formation of CLPs, it remains possible that GATA6 plays distinct cell-intrinsic roles in mediating the loss of B cells and pDCs from *Max41* mice that are separable from its role in early hematopoietic development.

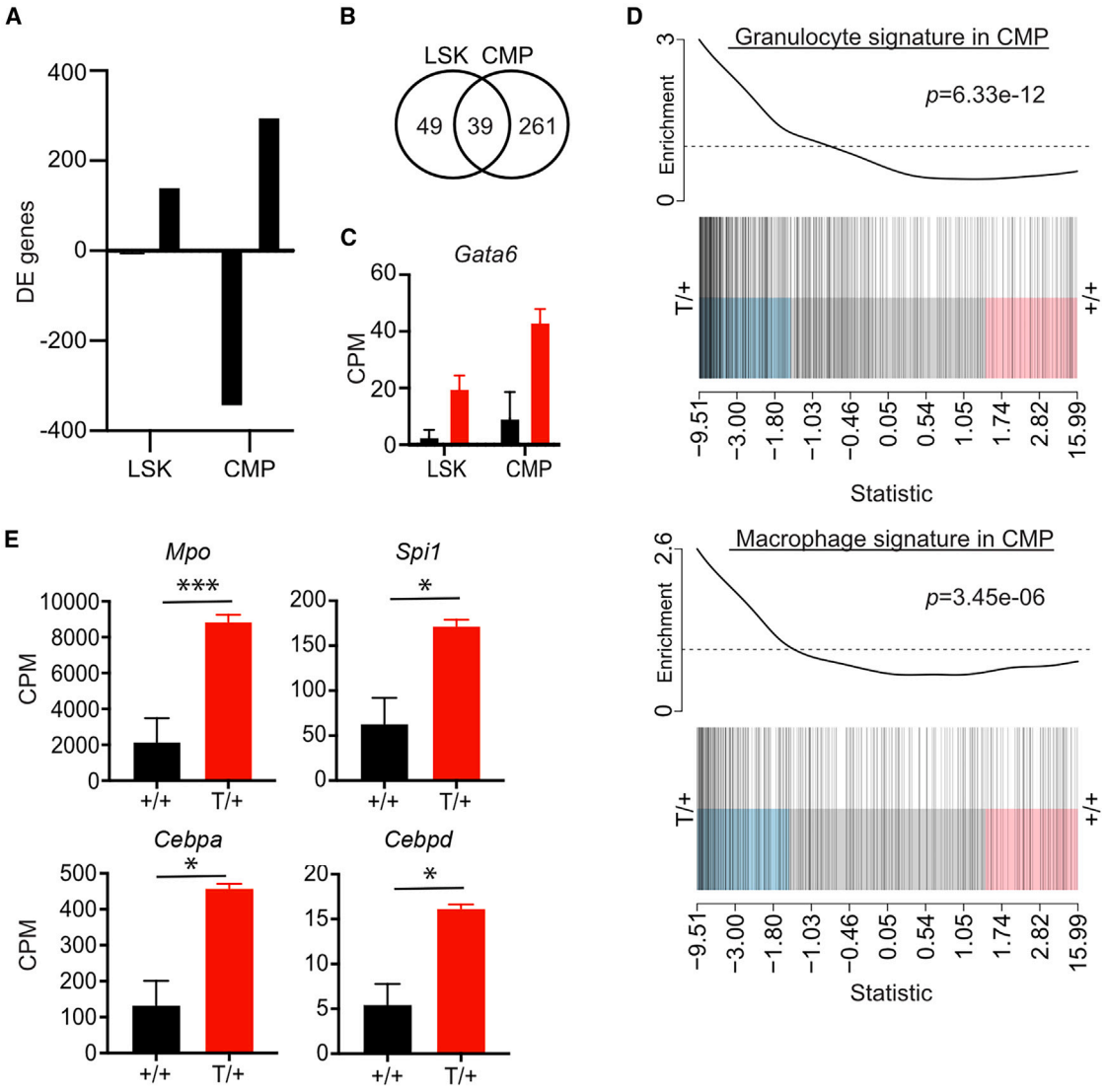

Figure 5. Mis-expression of *Gata6* in *Max41* bone marrow cells drives aberrant myeloid gene expression

(A) Determination of the number of genes differentially expressed (adjusted $p < 0.05$) between WT and *Max41*$^{T/+}$ LSK and CMP fractions ($n = 2$ for each cell population and genotype).

(B) Venn diagram showing the overlap between differentially expressed genes (from A) that are upregulated in WT LSKs and CMPs compared to the *Max41*$^{T/+}$ samples.

(C) Expression of *Gata6* in WT (black) and *Max41*$^{T/+}$(red) LSK and CMP fractions.

(D) Gene set enrichment analysis of genes (shaded rectangles horizontally ranked by moderated t-statistic) upregulated (pink), downregulated (blue), or not altered (gray) in WT CMPs relative to *Max41*$^{T/+}$ CMPs. Vertical lines indicate the position of signature genes for granulocytes (top) or macrophages (bottom). The worm shows the relative local enrichment of signature genes in each part of the plot, with the dotted horizontal line indicating neutral enrichment. The signatures were strongly upregulated in *Max41*$^{T/+}$ CMPs, with the *p* value indicating the result of a camera test. Signatures were obtained from http://haemosphere.org.[23]

(E) Expression of the indicated genes in WT (black) and *Max41*$^{T/+}$(red) CMPs. ***adjusted $p < 0.001$, *adjusted $p < 0.05$.

Data in (C) and (E) are the mean ± SD and derive from (A). CPM, counts per million reads. See also Figure S4.

STAR★METHODS

Detailed methods are provided in the online version of this paper and include the following:

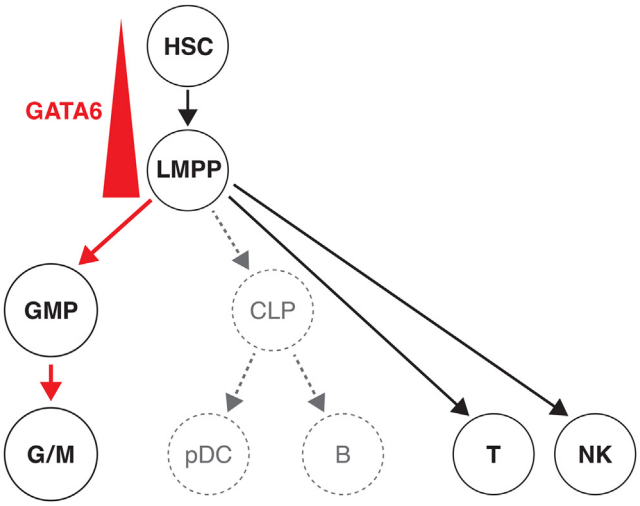

Figure 6. Model for the genetic basis of the *Max41* phenotype based upon changed progenitor populations

We suggest that, in WT mice, transition of a multipotent progenitor (MPP), such as LMPP, to the CLP stage requires downregulation of the *Gata1-2-3* genes. Aberrant upregulation of *Gata6* expression in *Max41* mice prevents this MPP-to-CLP transition, causing the absence of CLPs, B cells, and pDCs without affecting the numbers of T cells and NK cells. This demonstrates that CLPs are the main precursors of B cells and pDCs but not T cells and NK cells. The increased frequency of the transgenic CMP population is likely due to the upregulated expression by GATA6 of genes commonly associated with myeloid development.

SUPPLEMENTAL INFORMATION

Supplemental information can be found online at https://doi.org/10.1016/j.celrep.2024.114159.

ACKNOWLEDGMENTS

We thank J. Martin, L. Spencer, T. Kapitelli, and G. Siciliano for animal care and expertise; Dr. M. Herold, J. Stanley, L. Tai, F. Watson, and A. Morcom for the generation of CRISPR genetically altered mice; Dr. C. de Graaf for gene signature lists; and Drs. N. Jenkins, N. Copeland, G. Lindeman, A. Ng, T. Johanson, W. Alexander, and S. Chappaz for insightful discussions. This work was supported by the Australian NHMRC (program grant 461221, Research Fellowships 1042629, and 1196235, project grant 1127885, investigator grant 2026084, and Ideas grant 2000461), the Arthritis Australia Zimmer fellowship, and infrastructure support from the NHMRC (IRISS) and the Victorian State Government (OIS). Generation of genetically engineered mice used in this study was supported by the Australian Phenomics Network (APN) and the Australian Government through the National Collaborative Research Infrastructure Strategy (NCRIS) program.

AUTHOR CONTRIBUTIONS

Conceptualization, J.M.A., A.W.H., P.B., and M.C.; methodology, C.A., Y.L., J.N., A.K., and M.C.; investigation, C.A., Y.L., J.N., L.G., J.W.-A., P.B.-C., A.K., S.L.N., and M.C.; funding acquisition, J.M.A., P.B., S.N., S.L.N., and M.C.; supervision, J.M.A., P.B., S.L.N., and M.C.; writing – original draft, P.B. and M.C.; writing – review and editing, P.B., M.C., J.M.A., S.L.N., and A.S.

DECLARATION OF INTERESTS

The authors declare no competing interests.

Received: January 3, 2023
Revised: March 6, 2024
Accepted: April 11, 2024

REFERENCES

1. Iwasaki, H., and Akashi, K. (2007). Hematopoietic developmental pathways: on cellular basis. Oncogene *26*, 6687–6696. https://doi.org/10.1038/sj.onc.1210754.
2. Orkin, S.H., and Zon, L.I. (2008). Hematopoiesis: an evolving paradigm for stem cell biology. Cell *132*, 631–644. https://doi.org/10.1016/j.cell.2008.01.025.
3. Wilson, A., Laurenti, E., Oser, G., van der Wath, R.C., Blanco-Bose, W., Jaworski, M., Offner, S., Dunant, C.F., Eshkind, L., Bockamp, E., et al. (2008). Hematopoietic stem cells reversibly switch from dormancy to self-renewal during homeostasis and repair. Cell *135*, 1118–1129. https://doi.org/10.1016/j.cell.2008.10.048.
4. Kondo, M., Weissman, I.L., and Akashi, K. (1997). Identification of clonogenic common lymphoid progenitors in mouse bone marrow. Cell *91*, 661–672. https://doi.org/10.1016/s0092-8674(00)80453-5.
5. Akashi, K., Traver, D., Miyamoto, T., and Weissman, I.L. (2000). A clonogenic common myeloid progenitor that gives rise to all myeloid lineages. Nature *404*, 193–197. https://doi.org/10.1038/35004599.
6. Adolfsson, J., Månsson, R., Buza-Vidas, N., Hultquist, A., Liuba, K., Jensen, C.T., Bryder, D., Yang, L., Borge, O.J., Thoren, L.A.M., et al. (2005). Identification of Flt3+ lympho-myeloid stem cells lacking erythro-megakaryocytic potential a revised road map for adult blood lineage commitment. Cell *121*, 295–306. https://doi.org/10.1016/j.cell.2005.02.013.
7. Lindeman, G.J., Adams, J.M., Cory, S., and Harris, A.W. (1994). B-lymphoid to granulocytic switch during hematopoiesis in a transgenic mouse strain. Immunity *1*, 517–527.
8. Rodrigues, P.F., Alberti-Servera, L., Eremin, A., Grajales-Reyes, G.E., Ivanek, R., and Tussiwand, R. (2018). Distinct progenitor lineages contribute to the heterogeneity of plasmacytoid dendritic cells. Nat. Immunol. *19*, 711–722. https://doi.org/10.1038/s41590-018-0136-9.
9. Ghaedi, M., Steer, C.A., Martinez-Gonzalez, I., Halim, T.Y.F., Abraham, N., and Takei, F. (2016). Common-Lymphoid-Progenitor-Independent Pathways of Innate and T Lymphocyte Development. Cell Rep. *15*, 471–480. https://doi.org/10.1016/j.celrep.2016.03.039.
10. Carotta, S., Pang, S.H.M., Nutt, S.L., and Belz, G.T. (2011). Identification of the earliest NK-cell precursor in the mouse BM. Blood *117*, 5449–5452. https://doi.org/10.1182/blood-2010-11-318956.
11. Chen, Q., Ye, W., Jian Tan, W., Mei Yong, K.S., Liu, M., Qi Tan, S., Loh, E., Te Chang, K., Chye Tan, T., Preiser, P.R., and Chen, J. (2015). Delineation of Natural Killer Cell Differentiation from Myeloid Progenitors in Human. Sci. Rep. *5*, 15118. https://doi.org/10.1038/srep15118.
12. Cichocki, F., Grzywacz, B., and Miller, J.S. (2019). Human NK Cell Development: One Road or Many? Front. Immunol. *10*, 2078. https://doi.org/10.3389/fimmu.2019.02078.
13. Grzywacz, B., Kataria, N., Kataria, N., Blazar, B.R., Miller, J.S., and Verneris, M.R. (2011). Natural killer-cell differentiation by myeloid progenitors. Blood *117*, 3548–3558. https://doi.org/10.1182/blood-2010-04-281394.
14. D'Amico, A., and Wu, L. (2003). The early progenitors of mouse dendritic cells and plasmacytoid predendritic cells are within the bone marrow

hemopoietic precursors expressing Flt3. J. Exp. Med. *198*, 293–303. https://doi.org/10.1084/jem.20030107.

15. Sathe, P., Vremec, D., Wu, L., Corcoran, L., and Shortman, K. (2013). Convergent differentiation: myeloid and lymphoid pathways to murine plasmacytoid dendritic cells. Blood *121*, 11–19. https://doi.org/10.1182/blood-2012-02-413336.
16. Dress, R.J., Dutertre, C.A., Giladi, A., Schlitzer, A., Low, I., Shadan, N.B., Tay, A., Lum, J., Kairi, M.F.B.M., Hwang, Y.Y., et al. (2019). Plasmacytoid dendritic cells develop from Ly6D(+) lymphoid progenitors distinct from the myeloid lineage. Nat. Immunol. *20*, 852–864. https://doi.org/10.1038/s41590-019-0420-3.
17. Onai, N., Obata-Onai, A., Schmid, M.A., Ohteki, T., Jarrossay, D., and Manz, M.G. (2007). Identification of clonogenic common Flt3+M-CSFR+ plasmacytoid and conventional dendritic cell progenitors in mouse bone marrow. Nat. Immunol. *8*, 1207–1216. https://doi.org/10.1038/ni1518.
18. Naik, S.H., Sathe, P., Park, H.Y., Metcalf, D., Proietto, A.I., Dakic, A., Carotta, S., O'Keeffe, M., Bahlo, M., Papenfuss, A., et al. (2007). Development of plasmacytoid and conventional dendritic cell subtypes from single precursor cells derived in vitro and in vivo. Nat. Immunol. *8*, 1217–1226. https://doi.org/10.1038/ni1522.
19. Kueh, A.J., Pal, M., Tai, L., Liao, Y., Smyth, G.K., Shi, W., and Herold, M.J. (2017). An update on using CRISPR/Cas9 in the one-cell stage mouse embryo for generating complex mutant alleles. Cell Death Differ. *24*, 1821–1822. https://doi.org/10.1038/cdd.2017.122.
20. Tabula Muris Consortium; Overall coordination; Logistical coordination; Organ collection and processing; Library preparation and sequencing; Computational data analysis; Cell type annotation; Writing group; Supplemental text writing group; Principal investigators (2018). Single-cell transcriptomics of 20 mouse organs creates a Tabula Muris. Nature *562*, 367–372. https://doi.org/10.1038/s41586-018-0590-4.
21. Morrisey, E.E., Tang, Z., Sigrist, K., Lu, M.M., Jiang, F., Ip, H.S., and Parmacek, M.S. (1998). GATA6 regulates HNF4 and is required for differentiation of visceral endoderm in the mouse embryo. Genes Dev. *12*, 3579–3590. https://doi.org/10.1101/gad.12.22.3579.
22. Koutsourakis, M., Langeveld, A., Patient, R., Beddington, R., and Grosveld, F. (1999). The transcription factor GATA6 is essential for early extraembryonic development. Development *126*, 723–732.
23. Choi, J., Baldwin, T.M., Wong, M., Bolden, J.E., Fairfax, K.A., Lucas, E.C., Cole, R., Biben, C., Morgan, C., Ramsay, K.A., et al. (2019). Haemopedia RNA-seq: a database of gene expression during haematopoiesis in mice and humans. Nucleic Acids Res. *47*, D780–D785. https://doi.org/10.1093/nar/gky1020.
24. Avellino, R., and Delwel, R. (2017). Expression and regulation of C/EBPalpha in normal myelopoiesis and in malignant transformation. Blood *129*, 2083–2091. https://doi.org/10.1182/blood-2016-09-687822.
25. Rosenbauer, F., and Tenen, D.G. (2007). Transcription factors in myeloid development: balancing differentiation with transformation. Nat. Rev. Immunol. *7*, 105–117. https://doi.org/10.1038/nri2024.
26. Gautier, E.L., Ivanov, S., Williams, J.W., Huang, S.C.C., Marcelin, G., Fairfax, K., Wang, P.L., Francis, J.S., Leone, P., Wilson, D.B., et al. (2014). Gata6 regulates aspartoacylase expression in resident peritoneal macrophages and controls their survival. J. Exp. Med. *211*, 1525–1531. https://doi.org/10.1084/jem.20140570.
27. Okabe, Y., and Medzhitov, R. (2014). Tissue-specific signals control reversible program of localization and functional polarization of macrophages. Cell *157*, 832–844. https://doi.org/10.1016/j.cell.2014.04.016.
28. Rosas, M., Davies, L.C., Giles, P.J., Liao, C.T., Kharfan, B., Stone, T.C., O'Donnell, V.B., Fraser, D.J., Jones, S.A., and Taylor, P.R. (2014). The transcription factor Gata6 links tissue macrophage phenotype and proliferative renewal. Science *344*, 645–648. https://doi.org/10.1126/science.1251414.
29. Gao, J., Chen, Y.H., and Peterson, L.C. (2015). GATA family transcriptional factors: emerging suspects in hematologic disorders. Exp. Hematol. Oncol. *4*, 28. https://doi.org/10.1186/s40164-015-0024-z.
30. Heavey, B., Charalambous, C., Cobaleda, C., and Busslinger, M. (2003). Myeloid lineage switch of Pax5 mutant but not wild-type B cell progenitors by C/EBPalpha and GATA factors. EMBO J. *22*, 3887–3897. https://doi.org/10.1093/emboj/cdg380.
31. Feng, R., Desbordes, S.C., Xie, H., Tillo, E.S., Pixley, F., Stanley, E.R., and Graf, T. (2008). PU.1 and C/EBPalpha/beta convert fibroblasts into macrophage-like cells. Proc. Natl. Acad. Sci. USA *105*, 6057–6062. https://doi.org/10.1073/pnas.0711961105.
32. Laiosa, C.V., Stadtfeld, M., Xie, H., de Andres-Aguayo, L., and Graf, T. (2006). Reprogramming of committed T cell progenitors to macrophages and dendritic cells by C/EBP alpha and PU.1 transcription factors. Immunity *25*, 731–744. https://doi.org/10.1016/j.immuni.2006.09.011.
33. Allman, D., Sambandam, A., Kim, S., Miller, J.P., Pagan, A., Well, D., Meraz, A., and Bhandoola, A. (2003). Thymopoiesis independent of common lymphoid progenitors. Nat. Immunol. *4*, 168–174. https://doi.org/10.1038/ni878.
34. Balciunaite, G., Ceredig, R., Massa, S., and Rolink, A.G. (2005). A B220+ CD117+ CD19- hematopoietic progenitor with potent lymphoid and myeloid developmental potential. Eur. J. Immunol. *35*, 2019–2030. https://doi.org/10.1002/eji.200526318.
35. Cumano, A., Paige, C.J., Iscove, N.N., and Brady, G. (1992). Bipotential precursors of B cells and macrophages in murine fetal liver. Nature *356*, 612–615. https://doi.org/10.1038/356612a0.
36. Montecino-Rodriguez, E., Leathers, H., and Dorshkind, K. (2001). Bipotential B-macrophage progenitors are present in adult bone marrow. Nat. Immunol. *2*, 83–88. https://doi.org/10.1038/83210.
37. Yoshida, H., Lareau, C.A., Ramirez, R.N., Rose, S.A., Maier, B., Wroblewska, A., Desland, F., Chudnovskiy, A., Mortha, A., Dominguez, C., et al. (2019). The cis-Regulatory Atlas of the Mouse Immune System. Cell *176*, 897–912.e20. https://doi.org/10.1016/j.cell.2018.12.036.
38. Liao, Y., Smyth, G.K., and Shi, W. (2013). The Subread aligner: fast, accurate and scalable read mapping by seed-and-vote. Nucleic Acids Res. *41*, e108. https://doi.org/10.1093/nar/gkt214.
39. Liao, Y., Smyth, G.K., and Shi, W. (2014). featureCounts: an efficient general purpose program for assigning sequence reads to genomic features. Bioinformatics *30*, 923–930. https://doi.org/10.1093/bioinformatics/btt656.
40. Law, C.W., Chen, Y., Shi, W., and Smyth, G.K. (2014). voom: Precision weights unlock linear model analysis tools for RNA-seq read counts. Genome Biol. *15*, R29. https://doi.org/10.1186/gb-2014-15-2-r29.
41. Ritchie, M.E., Phipson, B., Wu, D., Hu, Y., Law, C.W., Shi, W., and Smyth, G.K. (2015). limma powers differential expression analyses for RNA-sequencing and microarray studies. Nucleic Acids Res. *43*, e47. https://doi.org/10.1093/nar/gkv007.
42. McCarthy, D.J., and Smyth, G.K. (2009). Testing significance relative to a fold-change threshold is a TREAT. Bioinformatics *25*, 765–771. https://doi.org/10.1093/bioinformatics/btp053.
43. Wu, D., and Smyth, G.K. (2012). Camera: a competitive gene set test accounting for inter-gene correlation. Nucleic Acids Res. *40*, e133. https://doi.org/10.1093/nar/gks461.

STAR★METHODS

KEY RESOURCES TABLE

REAGENT or RESOURCE	SOURCE	IDENTIFIER
Antibodies		
B220-A700	Biolegend	RA3-6B2 RRID:AB_493716
CD117-APC	WEHI Ab facility	ACK-4
CD11b-BV786	Biolegend	M1/70 RRID: AB_2561373
CD11c-BV510	Biolegend	N418 RRID:AB_2562010
CD127-biotin	WEHI Ab facility	A7R34
CD135-PE	eBioscience	A2F10 RRID:AB_465859
CD150-PECy7	Biolegend	TC15-12F12.2 RRID:AB_439796
CD16/32-BV605	BD Biosciences	2.4G2 RRID:AB_2737947
CD3-A700	WEHI Ab facility	17A2
CD34-FITC	BD Biosciences	RAM34 RRID:AB_1645242
CD48-PE	WEHI Ab facility	HM48.1
Gr1-A700	WEHI Ab facility	RB6-8c5
Sca1-A594	WEHI Ab facility	E13–161.7
Gr1-PE	WEHI Ab facility	RB6-8C5
TCRb-APC	eBioscience	H57-597 RRID: AB_469481
CD11b-ef450	eBioscience	M1/70 RRID:AB_1582236
CD19-BUV737	BD Biosciences	1D3 RRID:AB_2716867
Critical commercial assays		
Qiazol lysis reagent	Qiagen	Cat#79306
Tetro cDNA synthesis kit	Bioline	Cat#BIO-65042
iSCRIPT reverse transcription Supermix	Biorad	Cat#1708840
2x SensiFAST SYBR no-ROX Kit	Bioline	Cat#BIO-98005
TruSeq RNA Library Prep Kit v2	Illumina	Cat#FC-122-1001
RNeasy Micro kit	Qiagen	Cat#74004
CD117 MicroBeads, mouse - lyophilized	Miltenyi	Cat#130-097-146
Deposited data		
Raw and analyzed RNAseq data have been deposited in NCBI SRA	This study	BioProject ID: PRJNA1093667
Experimental models: Organisms/strains		
Max41 T/+ mice	Lindeman et al.[7]	N/A
Oligonucleotides		
Gata6-for 5′-CCAGCACAGACCTGTTGGA	This study	N/A
Gata6-rev 5′-GCTGTTACCGGAGCAAGCTT	This study	N/A
Rbbp8-for 5′-CGGATGCATCCAATGACTTCA	This study	N/A
Rbbp-8-rev 5′-CACATGCAAGCTCAGCTACTT	This study	N/A
Mib1-for 5′-GTCATGGAGGATGGACCGAT	This study	N/A
Mib1-rev 5′-CAGCAGCCTTAACCAGCTCTT	This study	N/A
Abhd3-for 5′-GCTGTGCGAACACTGAAGAC	This study	N/A
Abhd3-rev 5′-CACGTCGTCCGTAGCATTCA	This study	N/A
Gapdh-for 5′-AGGTCGGTGTGAACGGA TTTG	This study	N/A
Gapdh-rev 5′- TGTAGACCATGTAGTTGAGGTCA	This study	N/A
Software and algorithms		
R packages: Rsubread, edgeR, limma	Bioconductor	RRID: SCR_006442

(*Continued on next page*)

Continued

REAGENT or RESOURCE	SOURCE	IDENTIFIER
Flow Jo v10	Flo Jo, LLC	RRID: SCR_008520
Prism 9	GraphPad Software	RRID: SCR_002798
Other		
Immunological Genome Consortium ULI-RNAseq	Yoshida et al.[37]	http://rstats.immgen.org/Skyline/skyline.html
Tabula Muris Compendium	Tabula Muris Consortium et al.[20]	https://tabula-muris.ds.czbiohub.org
Haemopedia RNA-seq database	Choi et al.[23]	www.haemosphere.org

RESOURCE AVAILABILITY

Lead contact

Further information and requests for resources and reagents should be directed to and will be fulfilled by the lead contact, Andreas Strasser (strasser@wehi.edu.au)

Materials availability

The Max41 transgenic mice are available upon request.

Data and code availability

- RNA-seq data have been deposited in NCBI SRA and are publicly available as of the date of publication. Accession numbers are listed in the key resources table. The paper also analyses existing, publicly available data. The websites to access these datasets are listed in the key resources table.
- This paper does not report original code.
- Any additional information required to reanalyze the data reported in this work paper is available from the lead contact upon request.

EXPERIMENTAL MODEL AND STUDY PARTICIPANT DETAILS

Mice

Mice were produced and maintained on a C57BL/6 background and were analyzed between 6 and 12 weeks of age. Both male and female mice were used and no influence of the sex was noted. All animal experiments were conducted according to the guidelines of The Walter and Eliza Hall Institute Animal Ethics Committee.

METHOD DETAILS

Generation of the *Cldn15, Znhit1* and *Gata6* gene deletions

The MAGEC laboratory (WEHI) generated these mouse strains using previously published protocols.[19] Briefly, guide RNAs designed around the regions of interest were injected together with a recombinant CAS9 protein into fertilized one-cell stage embryos to promote DNA repair and homologous recombination. One-cell embryos were obtained by crossing *Max41* transgenic males with wt C57BL/6 females. Animals were screened for the intended genomic alterations by PCR and recombinant alleles were sequenced to confirm the desired genomic modifications. Subsequent crosses were carried out to produce mice of the genotypes of interest (Figure S6).

Flow cytometry

Spleens were minced and digested with 1 mg/mL type III collagenase (Worthington Biochemicals) and 0.0014 mg/mL DNase (Sigma-Aldrich) for 25 min at room temperature. Bone marrow was flushed from the femurs, tibias, and iliac crests. Digested spleen and bone marrow were passed through a 70-μm cell strainer (BD Biosciences) to yield single-cell suspensions prior to red blood cell lysis with NH_4Cl solution. Single cell suspensions were washed and resuspended in PBS+0.5% BSA (Sigma-Aldrich) and stained at 4°C. The list of the antibodies used in this study can be found in the Key Resources Table. All samples were acquired on a Fortessa X20 (BD Biosciences) and were analyzed with the FlowJo software (FlowJo, BD Biosciences). For sorting of the bone marrow HSPC, the cell suspension was first stained with CD117 MicroBeads (Miltenyi) following by a magnetic enrichment step as per the manufacturer's instruction before the staining. Cells were then sorted using a FACSAria III (BD Biosciences).

RT-PCR and oligonucleotides

Total RNA was extracted with Qiazol (Qiagen, Germantown, MD) according to the manufacturer's instructions. Five ug of total RNA were converted to cDNA using the Tetro cDNA synthesis kit (Bioline, Meridian bioscience, Memphis, Tennessee) in a 25 mL reaction.

Two mL of this reaction were used as template for the subsequent PCR reactions. The primers used in this study can be found in the Key Resources Table.

RT-QPCR

RNA was isolated using the RNeasy Plus Mini Kit, and cDNA was synthesized using iScript reverse transcription supermix (Bio-Rad). Amplification was performed by using the SYBR green master mix (Biolabs) on a Biorad CFX 384, using the *Gata6* and *Gapdh* primers found in the Key Resources Table.

Histology

Whole spleen and gently flushed bone marrow from 6 week old wt and *Max41*$^{T/+}$ mice were fixed in formalin overnight before being paraffin-embedded. 5 mm thick sections of embedded tissue were stained with Hematoxylin and Eosin (H&E) using standard procedures and stained slides were imaged using an Aperio Digital Pathology Slide Scanner.

Whole transcriptome analysis

RNA was isolated from *ex vivo* sorted bone marrow LSKs and CMPs from wt and *Max41*$^{T/+}$ mice using the Qiagen RNeasy Micro kit. Cell populations were sorted as shown in Figure S2. Libraries were generated using the Illumina Truseq RNA sample preparation kit following the manufacturer's instructions. Two biological replicates were generated and subjected to a transcriptome 75–100 bp single-end sequencing on an Illumina HiSeq 2500 instrument.

Sequencing reads were mapped to GRCm39 with Rsubread *align()* function,[38] and a gene x sample matrix was generated by Rsubread *featureCounts()* function.[39] The gene x sample matrix was further processed with the limma-voom pipeline for downstream analysis,[40,41] in which differentially expressed genes were called by using the limma *treat(lfc = log2(1.2))* function.[42] Gene set enrichment analysis was performed by using the limma *camera()* and *barcodeplot()* functions.[43] All immunoglobulin genes with differential expression were excluded.

Data availability

RNA-seq data from wt and *Max41*$^{T/+}$ LSKs and CMPs have been deposited in NCBI SRA (BioProject ID: PRJNA1093667), and can be accessed at https://www.ncbi.nlm.nih.gov/Traces/study/?acc=PRJNA1093667&o=acc_s%3Aa.

Analysis of publicly available gene expression datasets

Bulk RNA-seq data were generated by the Immunological Genome Project (ImmGen) using the ULI-seq technique and analyzed at http://rstats.immgen.org/Skyline/skyline.html.[37] Single cell RNA-seq data were from the Tabula Muris Compendium (https://tabula-muris.ds.czbiohub.org)[20]). Data were generated with SMART-seq2 on flow cytometrically sorted cells. Gene signatures for gene set enrichment analysis were derived from the Haemopedia RNA-seq database.[23]

QUANTIFICATION AND STATISTICAL ANALYSIS

Statistical analyses on non-transcriptomic data were carried out using unpaired Student's t-test with Welch's correction. All details for the non-RNAseq statistical analysis can be found in the figure legends. The analysis for the RNAseq data is described in the Methods.